

## Supplementary Information for

# Development of an Antibody-binding Modular Nanoplatfom for Antibody-guided Targeted Cell Imaging and Delivery

Hansol Kim, Young Ji Kang, Junseon Min, Hyeokjune Choi and Sebyung Kang\*

Department of Biological Sciences, School of Life Sciences, Ulsan National Institute of Science and Technology (UNIST), Ulsan, 689-798, Korea

## Supplementary figures

Fig. S1

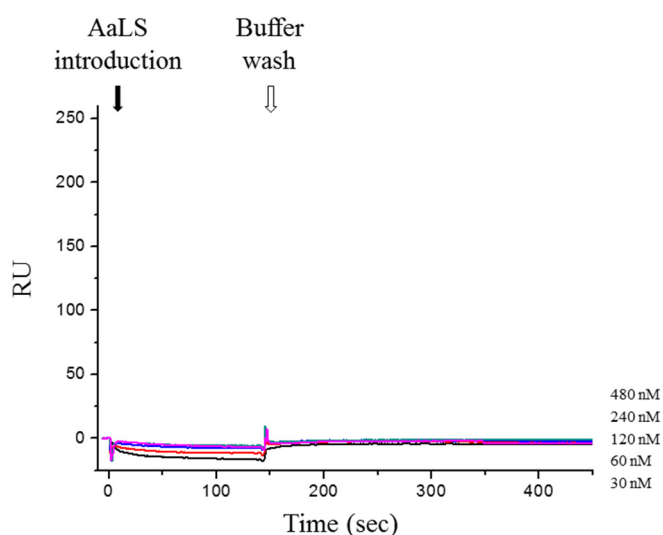


Fig. S1 SPR analyses of AaLS binding to rabbit IgG immobilized SPR gold sensors. Various amounts of AaLS (30, 60, 120, 240, and 480 nM) were loaded to the rabbit IgG immobilized SPR gold sensor at a flow rate of 5  $\mu$ l/min for 2 min (closed arrow) and subsequently buffers were added (open arrow) and kept flow for 8 min.

Fig. S2

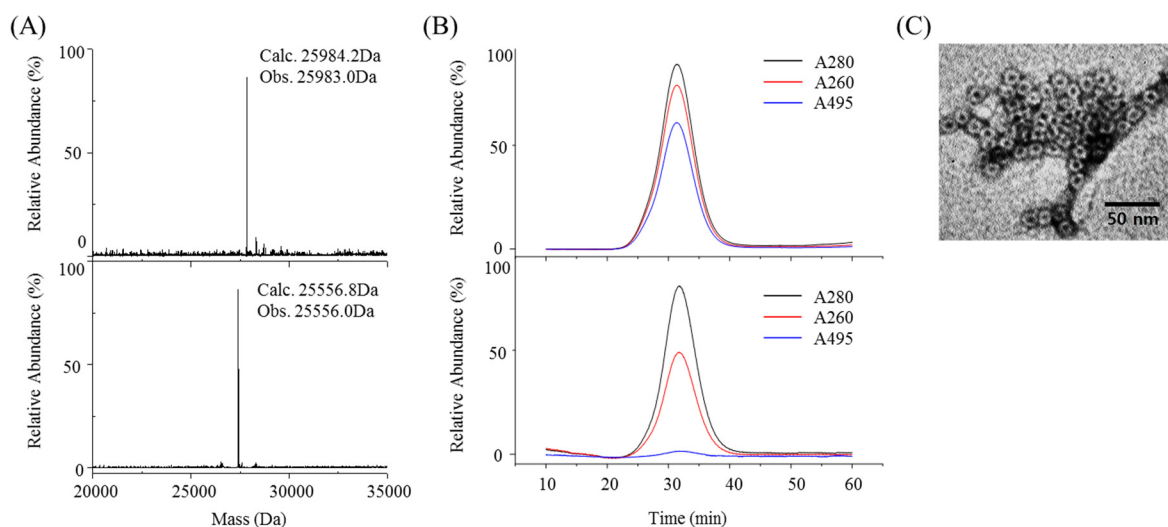


Fig. S2 Characterization of fluorescent dye (fluorescein) labeled ABD-AaLS (fABD-AaLS). (A) Molecular mass measurements of the dissociated subunits of ABD-AaLS (calc. 25556.8 Da; obs. 25557.0 Da, bottom) and fABD-AaLS (calc. 25984.2 Da; obs. 25983.0 Da, top). Molecular mass increase (427.0 Da) upon labeling agreed excellent with molecular mass of fluorescein-5-maleimide (427.4 Da) (B) Size exclusion elution profiles of ABD-AaLS (bottom) and fABD-AaLS (top). fABD-AaLS eluted same time as that of untreated ABD-AaLS. Significant absorption increase at 495 nm is due to the attached fluoresceins. (C) Transmission electron micrographic (TEM) image of 2% uranyl acetate stained fABD-AaLS. fABD-AaLS maintained its cage architecture even after chemical conjugation of fluorescein.

Fig. S3

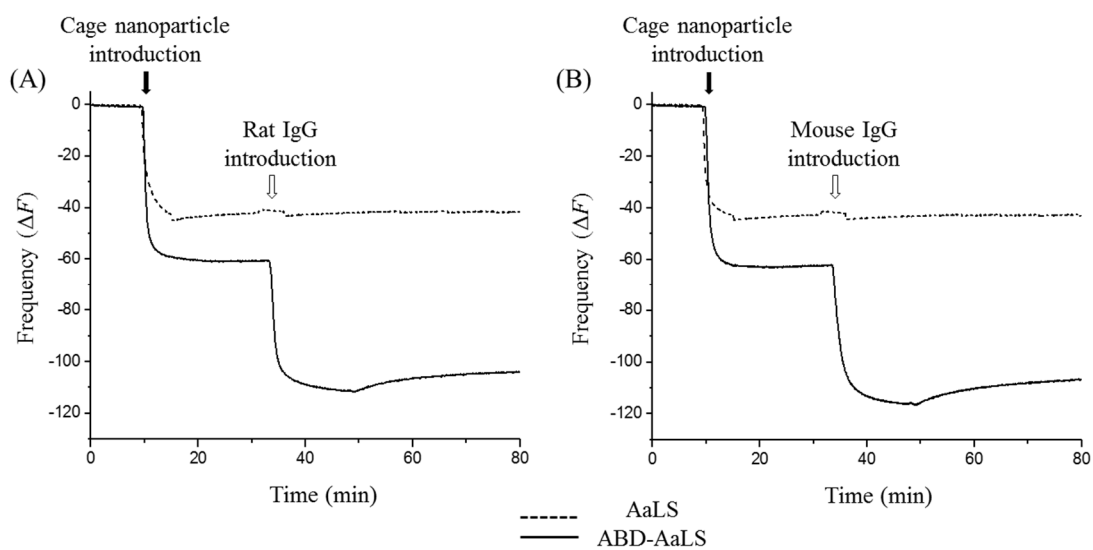


Fig. S3 QCM resonance signal changes ( $-\Delta F$ ) upon introductions of either AaLS (dashed line) or ABD-AaLS (solid line) onto the surface of standard gold sensors (closed arrow) and subsequent deposition of rat (A) or mouse (B) IgGs on the monolayers of either AaLS (dashed line) or ABD-AaLS (solid line) (open arrow).

Fig. S4

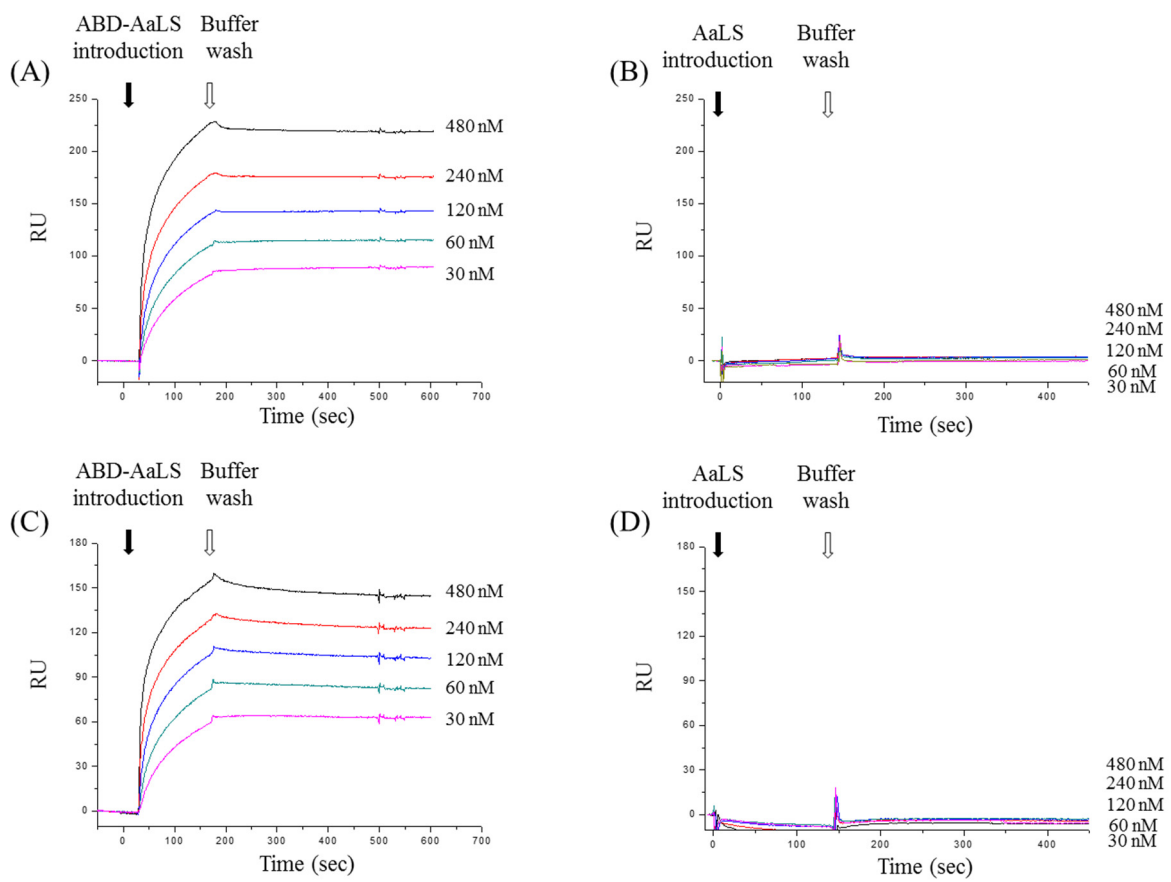


Fig. S4 SPR analyses of ABD-AaLS or AaLS binding to rat (A and B) or mouse (C and D) IgG immobilized SPR gold sensors. Various amounts of ABD-AaLS (A and C) or AaLS (B and D) (30, 60, 120, 240, and 480 nM) were loaded to the rat or mouse IgG immobilized SPR gold sensor at a flow rate of 5  $\mu$ l/min for 2 min (closed arrow) and subsequently buffers were added (open arrow) and kept flow for 8 min.

Fig. S5

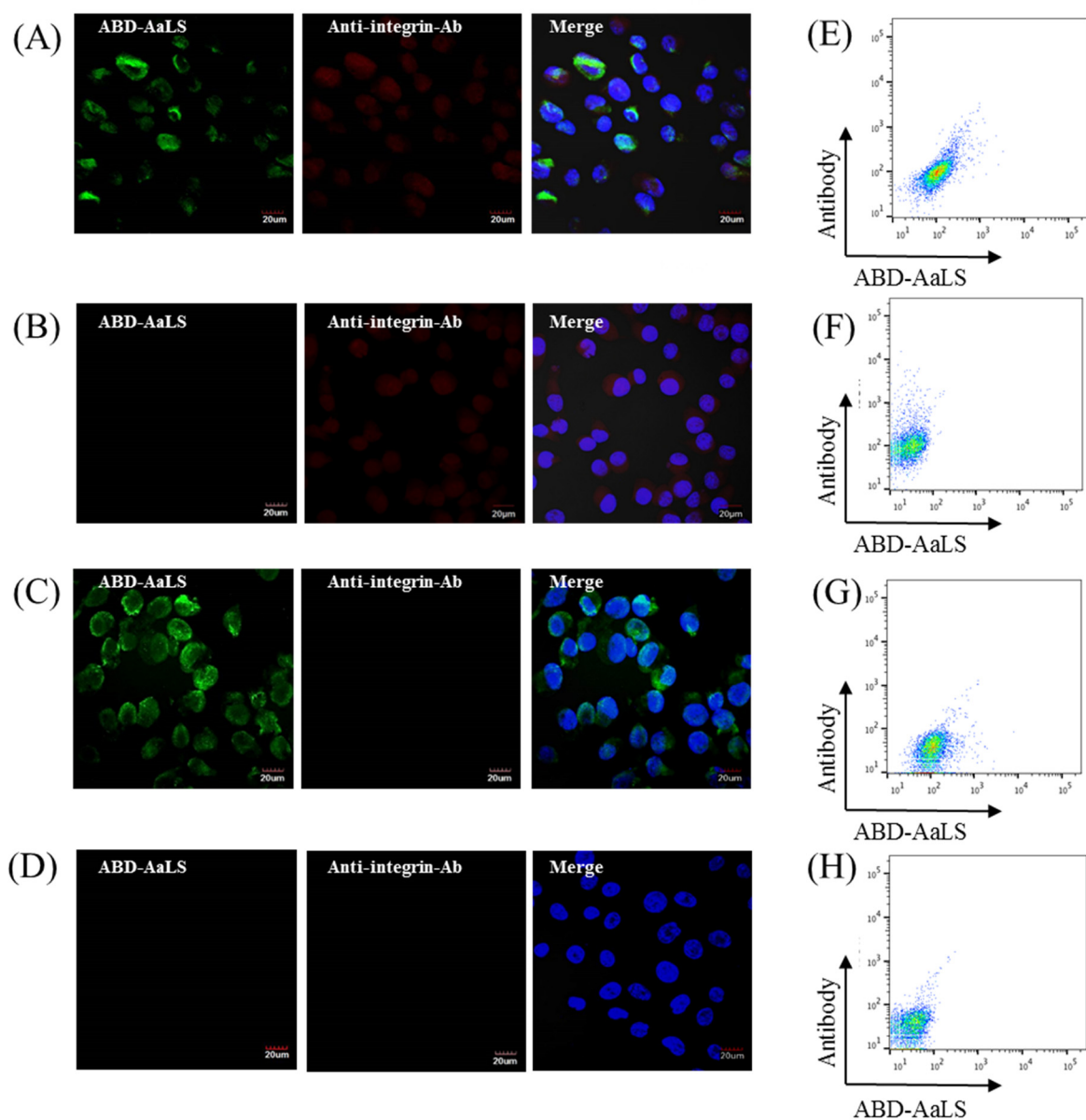


Fig. S5 Fluorescence microscopic images (A-D) and flow cytometry measurements (E-H) of KB cells treated with Alexa-integrin-Ab/fABD-AaLS complexes (A and E), Alexa-integrin-Ab only (B and F), integrin-Ab/fABD-AaLS complexes (C and G) and fABD-AaLS only (D and H), respectively. Mouse anti-integrin IgG and ABD-AaLS were labeled with Alexa-647 (Alexa-CD44-Ab, red) and fluorescein (fABD-AaLS, green), respectively, and nuclei were visualized with DAPI as blue. Fluorescein (left rows), Alexa-647 (middle rows), and merged with DAPI staining (right rows) were presented.

Fig. S6

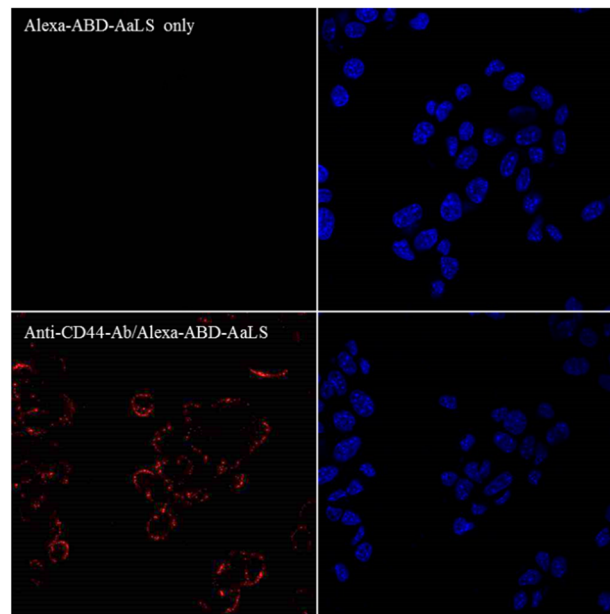


Fig. S6 Florescent microscopic images of SCC-7 cells treated with Alexa-ABD-AaLS only (top two panels) and CD44-Ab/Alexa-ABD-AaLS complexes (bottom two panels), respectively. ABD-AaLS were labeled with Alexa-647 (Alexa-ABD-AaLS, red) and nuclei were visualized with DAPI as blue, whereas rat anti-CD44 IgG was not labeled with any dyes at all. Alexa-647 (left rows) and DAPI staining (right rows) were presented.